1498 *Inorg. Chem.* **2011**, *50*, 1498–1505
DOI: 10.1021/ic102117d

Inorganic Chemistry
Article

Complexation, Computational, Magnetic, and Structural Studies of the Maillard Reaction Product Isomaltol Including Investigation of an Uncommon π Interaction with Copper(II)

Katja B. Heine,[†,‡] Jack K. Clegg,[§] Axel Heine,[†] Kerstin Gloe,[†] Karsten Gloe,[*,†] Thomas Henle,[*,†] Gert Bernhard,[‡] Zheng-Li Cai,[§] Jeffrey R. Reimers,[§] Leonard F. Lindoy,[*,§] Jochen Lach,[⊥] and Berthold Kersting[⊥]

[†]*Department of Chemistry and Food Chemistry, TU Dresden, 01062 Dresden, Germany,* [§]*School of Chemistry, University of Sydney, New South Wales 2006, Australia,* [‡]*Institute of Radiochemistry, Helmholtz Center Dresden−Rossendorf, 01314 Dresden, Germany, and* [⊥]*Institute of Inorganic Chemistry, University of Leipzig, 04103 Leipzig, Germany*

Received October 20, 2010

The metal complexation properties of the naturally occurring Maillard reaction product isomaltol **HL²** are investigated by measurement of its stability constants with copper(II), zinc(II), and iron(III) using potentiometric pH titrations in water, by structural and magnetic characterization of its crystalline complex, $[Cu(\mathbf{L^2})_2]\cdot 8H_2O$, and by density functional theory calculations. Strong complexation is observed to form the bis(isomaltolato)copper(II) complex incorporating copper in a typical (pseudo-)square-planar geometry. In the solid state, extensive intra- and intermolecular hydrogen bonding involving all three oxygen functions per ligand assembles the complexes into ribbons that interact to form two-dimensional arrays; further hydrogen bonds and π interactions between the furan moiety of the anionic ligands and adjacent copper(II) centers connect the complexes in the third dimension, leading to a compact polymeric three-dimensional (3D) arrangement. The latter interactions involving copper(II), which represent an underappreciated aspect of copper(II) chemistry, are compared to similar interactions present in other copper(II) 3D structures showing interactions with benzene molecules; the results indicate that dispersion forces dominate in the π system to chelated copper(II) ion interactions.

Introduction

Maillard reaction products (MRPs) are formed by nonenzymatic reactions between reducing sugars and proteins or amino acids and appear both in food and in vivo. This reaction may lead to low-molecular-weight flavor compounds as well as to high-molecular-weight polymers, which are responsible for food browning. The relevance of the Maillard reaction in food and in vivo and its resulting physiological consequences have been the subject of several reviews in the last years.[1−3]

Despite the widely accepted commercial and biochemical roles of MRPs, the number of papers describing the interaction of defined compounds with metal ions and their consequences remains limited.[4−6] A number of studies have documented the influence of MRPs on metal ions in vivo. For example, it has been demonstrated that, in general, rats excrete an increased amount of zinc(II) after their diets are enriched with MRPs.[7] However, related studies of the influence of MRPs on the copper(II) balance have shown opposing results. Rehner and Walter[8] found an increase in renal excretion of copper(II), whereas Delgado-Andrade et al.[9] reported a decrease in both renal and fecal copper(II) excretion.

The first report presenting the stability constants of selected MRPs with biologically relevant metal ions [magnesium(II), calcium(II), copper(II), and zinc(II)] was published by O'Brien and Morrissey.[5] It was found that fructosyl glycine shows a lower binding of zinc(II) ($\log K_1$ = 4.27, $\log K_2$ = 3.83, and $\log K_3$ = 1.92) than glycine ($\log K_1$ = 5.40, $\log K_2$ = 4.47, and $\log K_3$ = 2.73).[5] In a more recent work, Seifert et al. investigated the complex formation of the

*To whom correspondence should be addressed. E-mail: Karsten.Gloe@chemie.tu-dresden.de (K.G.), Thomas.Henle@chemie.tu-dresden.de (T.H.), L.Lindoy@chem.usyd.edu.au (L.F.L.).

(1) Gerrard, J. A. *Aust. J. Chem.* **2002**, *55*, 299–310.
(2) Nursten, H. The Maillard Reaction: Chemistry. *Biochemistry and Implications*; RSC: Cambridge, U.K., 2005.
(3) Finot, P.-A. *Ann. N.Y. Acad. Sci.* **2005**, *1043*, 1–8.
(4) Ramonaityte, D. T.; Kersiene, M.; Adams, A.; Tehrani, K. A.; De Kimpe, N. *Food Res. Int.* **2009**, *42*, 331–336.
(5) O'Brien, J.; Morrissey, P. A. *Food Chem.* **1997**, *58*, 17–27.
(6) Seifert, S. T.; Krause, R.; Gloe, K.; Henle, T. *J. Agric. Food Chem.* **2004**, *52*, 2347–2350.
(7) Finot, P. A.; Furniss, D. E. *Prog. Clin. Biol. Res.* **1989**, *304*, 343–358.
(8) Rehner, G.; Walter, T. *Z. Ernährungswiss.* **1991**, *30*, 50–55.
(9) Delgado-Andrade, C.; Seiquer, I.; Navarro, M. P. *J. Sci. Food Agric.* **2004**, *84*, 1507–1513.

 Published on Web 01/26/2011

MRPs N^{α}-hippuryl-N^{ε}-fructoselysine and N^{α}-hippuryl-N^{ε}-carboxymethyllysine with zinc(II) and copper(II).[6] Whereas the complex formation of both with zinc(II) was not able to be observed, the constants for copper(II) were determined as $\log K_1 = 5.8$ and $\log K_2 = 4.0$ for N^{α}-hippuryl-N^{ε}-fructoselysine and $\log K_1 = 7.3$ and $\log K_2 = 6.3$ for N^{α}-hippuryl-N^{ε}-carboxymethyllysine.[6]

Although a detailed description of the complexation behavior of important MRPs in living systems is of fundamental importance to the understanding of health-related interactions as well as to the development of well-characterized systems in which such products are to be used and handled, e.g., tris(maltolato)iron(III) for the therapeutic treatment of iron deficiency anemia in individuals,[10,11] obtaining a detailed knowledge of the structural aspects and complexing properties of such systems has proved especially challenging. Typical ligands in question are the pyrone derivative maltol **HL^1** and its structural isomer isomaltol **HL^2** (Scheme 1). However, in vitro studies have demonstrated that these potentially bidentate oxygen-donor ligands show pronounced complexation abilities toward a range of metal ions, typically forming neutral chelates of the general composition ML_n that incorporate five- and six-membered chelate rings, respectively.[12−16]

Isomaltol (**HL^2**) was first isolated and studied in 1910 by Backe, who demonstrated its complexation affinity for iron(III) and copper(II).[17] However, the structure of isomaltol was only assigned in 1964 using spectroscopic data,[18] and up to now, the coordination chemistry of isomaltol has received much less attention than that of its isomer maltol **HL^1**. In part, this may reflect the lower basicity of the isomaltolato anion and its resulting weaker complexation tendency.[12−16] The protonation constant for **HL^2** and its stability constants with beryllium(II), aluminum(III), gallium(III), indium(III), vanadium(III), and vanadium(IV) have been reported previously, together with the structures of the corresponding $[Be(\mathbf{L^2})_2]$, $[Al(\mathbf{L^2})_3]$, $[V(\mathbf{L^2})_3]$, and $[VO(\mathbf{L^2})_2(H_2O)]$ complexes.[14−16]

As part of our investigation of the formation and identification of MRPs in food[19] and the characterization of their metal complexation capabilities,[6] we now report the complex stability constants for the interaction of isomaltol **HL^2** with copper(II), zinc(II), and iron(III) and the X-ray crystal structures of the free ligand and its copper(II) complex. Furthermore, the magnetic behavior of the isolated copper(II) complex has been characterized. Computational studies on the latter aimed at investigating a little studied intermolecular interaction type[20−22] involving π interaction between the furan ring of the complexed isomaltolate anion and adjacent copper(II) centers are also presented.

Scheme 1

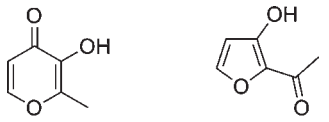

HL^1 **HL^2**

Experimental Section

Materials. All reagents and solvents were obtained commercially and used without further purification. Water was boiled to remove carbon dioxide and stored under argon.

Isomaltol, HL^2. This was prepared from *O*-galactosyl isomaltol using a slight modification of the literature procedure.[16,23,24] *O*-Galactosyl isomaltol was obtained by the reaction of α-D-lactose with piperidine, glacial acetic acid, and triethylamine in ethanol under reflux. After standing in an ice bath for 1 h and dilution with ethanol, the solid product was isolated by vacuum filtration. Isomaltol was sublimed from the reaction mixture in a sealed ampule at 240 °C. The crude solid was washed with ice water and dried under vacuum; yield 82% (based on *O*-galactosyl isomaltol). Crystals of **HL^2** suitable for X-ray structural analysis were obtained by the slow evaporation of a methanol/acetone solution of this product. Characterization data were in agreement with those reported previously.[16,23,24]

Bis(isomaltolato)copper(II), $[Cu(\mathbf{L^2})_2]\cdot 8H_2O$. $CuSO_4\cdot 5H_2O$ (81.0 mg, 0.32 mmol) was dissolved in water (7 mL) containing dissolved **HL^2** (39.45 mg, 0.31 mmol) to yield a light-green solution. After 2 days, moss-green crystals had formed. For the X-ray study, a crystal was removed directly from the reaction solution; its water content corresponds to that of $[Cu(\mathbf{L^2})_2]\cdot 8H_2O$. For elemental analysis, crystals were isolated, washed with diethyl ether, and dried in air, which led to a loss of water, resulting in a composition of $[Cu(\mathbf{L^2})_2]\cdot 1.8H_2O$. Yield: 12.5 mg (0.04 mmol; 26% based on **HL^2**). ESI-MS: m/z 187.8 $[Cu(\mathbf{L^2})]^+$, 313.9 $[Cu(\mathbf{L^2})_2 + H]^+$. Found: C, 40.80; H, 3.19. Calcd.: C, 41.63; H, 3.96. IR (cm^{-1}, KBr disk): 1581, 1548, 1514 ($\nu_{C=O}$, $\nu_{C=C}$), 441 (ν_{Cu-O}).

Potentiometric pH Titrations. Potentiometric stability constant measurements were carried out at 298.0 ± 0.1 K at an ionic strength of 0.15 M (KNO_3). The redetermination of the protonation constant of isomaltol was performed with a 736 GP Titrino unit from Metrohm (Herisau, Switzerland) under a carbon dioxide-free, moist nitrogen atmosphere. The calibration of the combined LL-micro pH electrode (Metrohm; Herisau, Switzerland) was performed by means of a HNO_3 (15 mM) titration. The calibration constants, the concentration of the base, and its carbon dioxide content were calculated using the computer software *GLEE*.[25] All quoted equilibrium constants are concentration constants. A pK_w value of 13.77 was used for the calculations, and all determinations were obtained under identical conditions.[6]

(10) Harvey, R. S. J.; Reffitt, D. M.; Doig, L. A.; Meenan, J.; Ellis, R. D.; Thompson, R. P. H.; Powell, J. J. *Aliment. Pharmacol. Ther.* **1998**, *12*(9), 845–848.
(11) Reffitt, D. M.; Burden, T. J.; Seed, P. T.; Wood, J.; Thompson, R. P. H.; Powell, J. J. *Ann. Clin. Biochem.* **2000**, *37*(4), 457–466.
(12) Thompson, K. H.; Barta, C. A.; Orvig, C. *Chem. Soc. Rev.* **2006**, *35*, 545–556.
(13) Antipova, I. A.; Mukha, S. A.; Medvedeva, S. A. *Russ. Chem. Bull.* **2004**, *53*, 780–784.
(14) Cecconi, F.; Ghilardi, C. A.; Lenco, A.; Mariani, P.; Mealli, C.; Midollini, S.; Orlandini, A.; Vacca, A. *Inorg. Chem.* **2002**, *41*, 4006–4017.
(15) Lutz, T. G.; Clevette, D. J.; Rettig, S. J.; Orvig, C. *Inorg. Chem.* **1989**, *28*, 715–719.
(16) Saatchi, K.; Thompson, K. H.; Patrick, B. O.; Pink, M.; Yuen, V. G.; McNeill, J. H.; Orvig, C. *Inorg. Chem.* **2005**, *44*, 2689–2697.
(17) (a) Backe, A. *Compt. Rend.* **1910**, *151*, 78–80. (b) Backe, A. *Compt. Rend.* **1910**, *150*, 540–543.
(18) Fisher, B. E.; Hodge, J. E. *J. Org. Chem.* **1964**, *29*, 776–781.
(19) (a) Henle, T. *Amino Acids* **2005**, *29*, 313–322. (b) Henle, T. *Mol. Nutr. Food Res.* **2007**, *51*, 1075–1078.
(20) Hori, A.; Arii, T. *CrystEngComm* **2007**, *9*, 215–217.
(21) Michalska, D.; Hernik, K.; Wysokiński, R.; Morzyk-Ociepa, B.; Pietraszko, A. *Polyhedron* **2007**, *26*, 4303–4313.
(22) Helios, K.; Wysokinski, R.; Zierkiewicz, W.; Proniewicz, L. M.; Michalska, D. *J. Phys. Chem. B* **2009**, *113*, 8158–8169.
(23) Hodge, J. E.; Nelson, E. C. *Cereal Chem.* **1961**, *38*, 207–221.
(24) Fox, R. C.; Taylor, P. D. *Synth. Commun.* **1999**, *29*, 989–1001.
(25) Gans, P.; O'Sullivan, B. *Talanta* **2000**, *51*, 33–37.

Three titrations per sample were performed for each stability constant determination. During the titrations, KOH (0.2 M) was added incrementally to 9 mL of a solution of HNO_3 (15 mM) and $\mathbf{HL^2}$ [3 mM in the absence of the metal ion and 1 mM in the presence of zinc(II) and 0.5 mM for copper(II)]. The titrations were performed at metal ion to ligand ratios of 1:1 and 1:2. The ionic strength was maintained by using the required amount of an electrolytic solution. The concentrations of the stock solutions of the metal nitrates and the acid were checked by titration against ethylenediaminetetraacetic acid or against tris(hydroxymethyl)aminomethane, respectively.

The titration data were recorded using the computer software *Vesuv 3.0* (Metrohm; Herisau, Switzerland); the stability constants were calculated using *HYPERQUAD*.[26]

The formation constants β_{mlh} are given by

$$m\mathrm{M} + l\mathrm{L} + h\mathrm{H} \xrightarrow{\beta_{mlh}} \mathrm{M}_m\mathrm{L}_l\mathrm{H}_h$$

with

$$\beta_{mlh} = \frac{[\mathrm{M}_m\mathrm{L}_l\mathrm{H}_h]}{[\mathrm{M}]^m[\mathrm{L}]^l[\mathrm{H}]^h}$$

where M is the metal ion, L the deprotonated ligand, and H the proton.

For the protonation of a complex or the attachment of another ligand molecule to an existing complex, the constants K_{h+1} and K_{l+1} are given by

$$\mathrm{M}_m\mathrm{L}_l\mathrm{H}_h + \mathrm{H} \xrightarrow{K_{h+1}} \mathrm{M}_m\mathrm{L}_l\mathrm{H}_{h+1}$$

with

$$K_{h+1} = \frac{[\mathrm{M}_m\mathrm{L}_l\mathrm{H}_{h+1}]}{[\mathrm{M}_m\mathrm{L}_l\mathrm{H}_h][\mathrm{H}]}$$

and

$$\mathrm{M}_m\mathrm{L}_l + \mathrm{L} \xrightarrow{K_{l+1}} \mathrm{M}_m\mathrm{L}_{l+1}$$

with

$$K_{l+1} = \frac{[\mathrm{M}_m\mathrm{L}_{l+1}]}{[\mathrm{M}_m\mathrm{L}_l][\mathrm{L}]}$$

Complexes with hydroxides are described using a negative value for h. Species distributions were obtained using *HYSS*.[27]

X-ray Crystallography. The data were collected with a Nonius Kappa CCD employing graphite-monochromated Mo Kα radiation generated from a sealed tube (0.710 73 Å) with φ and ω scans to approximately 56° 2θ at 198(2) K. Data collections were undertaken with *COLLECT*,[28] cell refinement with *Dirax/lsq*,[29] and data reduction with *EvalCCD*.[30] Subsequent computations for all data were carried out using the *WinGX-32* graphical user interface.[31] Structures were solved by direct methods using *SIR97*.[32] Multiscan empirical absorption corrections were applied to data sets using the program *SADABS*.[33] Data were refined and extended with *SHELXL-97*.[34] All non-hydrogen atoms were refined anisotropically. Carbon-bound hydrogen atoms were included in idealized positions and refined using a riding model. Oxygen-bound hydrogen atoms were first located in the difference Fourier map before refinement. Some hydrogen atoms attached to the water molecules of crystallization in $[\mathrm{Cu}(\mathbf{L^2})_2]\cdot 8\mathrm{H_2O}$ were disordered and modeled with bond-length and angle restraints. Data are summarized in Table S1 in the Supporting Information.

Electronic Structure Calculations. The π interactions between copper(II) ions and the furan-based ligand $\mathbf{HL^2}$, benzene, and the model ligand $\mathbf{HL^3}$ were investigated using density functional theory (DFT). All calculations were performed by *Gaussian 09*[35] using the dispersion-corrected B97D density functional[36] with the SDD+ basis set[37] for copper and the 6-31+G* basis set[20,38] for all other atoms. Basis-set superposition errors (BSSEs) were accounted for by using the counterpoise method applied only at the final optimized geometries. The basis set used is sufficiently large that the BSSE is not expected to affect geometry optimization. The use of a dispersion-corrected density functional is essential because dispersion is very important for the interaction of aromatic molecules with copper surfaces[39] and has been shown to be crucial for a similar copper(II)−π interaction.[22] A cluster-based approach was applied rather than one involving crystallographic boundary conditions owing to the ready availability of dispersion-corrected density functionals in codes such as *Gaussian*.

Magnetic Measurements. The susceptibility measurements were carried out using a MPMS 7XL SQUID magnetometer by Quantum Design at an applied external field of 1 T in a temperature range of 2−371 K.

Results and Discussion

Structure of Isomaltol $\mathbf{HL^2}$. Small yellow platelike crystals of isomaltol suitable for diffraction studies were obtained by the slow evaporation of this product from a methanol/acetone solution. The molecular structure (Figure 1) shows a planar arrangement reflecting the broad sp^2 hybridization in the molecule. As was already demonstrated by spectroscopic studies,[18] $\mathbf{HL^2}$ adopts a configuration with the ketone group [O(6)] on the same side of the molecule as the furan oxygen [O(1)].

(26) Gans, P.; Sabatini, A.; Vacca, A. *Talanta* **1996**, *43*, 1739–1753.
(27) Alderighi, L.; Gans, P.; Ienco, A.; Peters, D.; Sabatini, A.; Vacca, A. *Coord. Chem. Rev.* **1999**, *184*, 311–318.
(28) *COLLECT*; Nonius BV: Delft, The Netherlands, 1998.
(29) Duisenberg, A. J. M. *J. Appl. Crystallogr.* **1992**, *25*, 92–96.
(30) Duisenberg, A. J. M.; Kroon-Batenburg, L. M. J.; Schreurs, A. M. M. *J. Appl. Crystallogr.* **2003**, *36*, 220–229.
(31) Farrugia, L. J. *J. Appl. Crystallogr.* **1999**, *32*, 837–838.
(32) Altomare, A.; Burla, M. C.; Camalli, M.; Cascarano, G. L.; Giacovazzo, C.; Guagliardi, A.; Moliterni, A. G. G.; Polidori, G.; Spagna, R. *J. Appl. Crystallogr.* **1999**, *32*, 115–119.
(33) Sheldrick, G. M. *SADABS*; University of Göttingen: Göttingen, Germany, 2002.
(34) Sheldrick, G. M. *SHELX-97*; University of Göttingen: Göttingen, Germany, 1997.
(35) Gaussian 09, revision A.02, Frisch, M. J.; Trucks, G. W.; Schlegel, H. B.; Scuseria, G. E.; Robb, M. A.; Cheeseman, J. R.; Scalmani, G.; Barone, V.; Mennucci, B.; Petersson, G. A.; Nakatsuji, H.; Caricato, M.; Li, X.; Hratchian, H. P.; Izmaylov, A. F.; Bloino, J.; Zheng, G.; Sonnenberg, J. L.; Hada, M.; Ehara, M.; Toyota, K.; Fukuda, R.; Hasegawa, J.; Ishida, M.; Nakajima, T.; Honda, Y.; Kitao, O.; Nakai, H.; Vreven, T.; Montgomery, Jr., J. A.; Peralta, J. E.; Ogliaro, F.; Bearpark, M.; Heyd, J. J.; Brothers, E.; Kudin, K. N.; Staroverov, V. N.; Kobayashi, R.; Normand, J.; Raghavachari, K.; Rendell, A.; Burant, J. C.; Iyengar, S. S.; Tomasi, J.; Cossi, M.; Rega, N.; Millam, N. J.; Klene, M.; Knox, J. E.; Cross, J. B.; Bakken, V.; Adamo, C.; Jaramillo, J.; Gomperts, R.; Stratmann, R. E.; Yazyev, O.; Austin, A. J.; Cammi, R.; Pomelli, C.; Ochterski, J. W.; Martin, R. L.; Morokuma, K.; Zakrzewski, V. G.; Voth, G. A.; Salvador, P.; Dannenberg, J. J.; Dapprich, S.; Daniels, A. D.; Farkas, Ö.; Foresman, J. B.; Ortiz, J. V.; Cioslowski, J.; Fox, D. J. Gaussian, Inc., Wallingford CT, 2009.
(36) Grimme, S. *J. Comput. Chem.* **2006**, *27*, 1787–1799.
(37) Andrae, D.; Häussermann, U.; Dolg, M.; Stoll, H.; Preuss, H. *Theor. Chim. Acta* **1990**, *77*, 123–141.
(38) Hehre, W. J.; Ditchfield, R.; Pople, J. A. *J. Chem. Phys.* **1972**, *56*, 2257–2261.
(39) Bilic, A.; Reimers, J. R.; Hush, N. S.; Hoft, R. C.; Ford, M. J. *J. Chem. Theory Comput.* **2006**, *2*, 1093–1105.

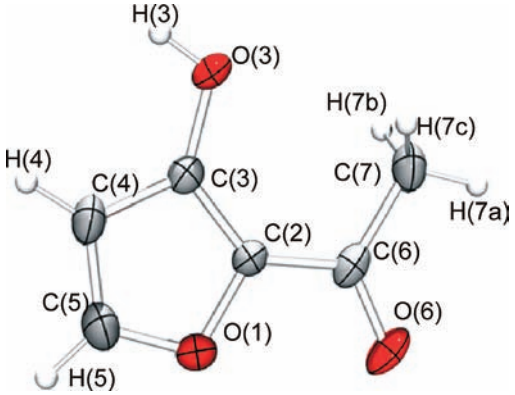

Figure 1. ORTEP representation of the isomaltol structure showing 50% probability ellipsoids.

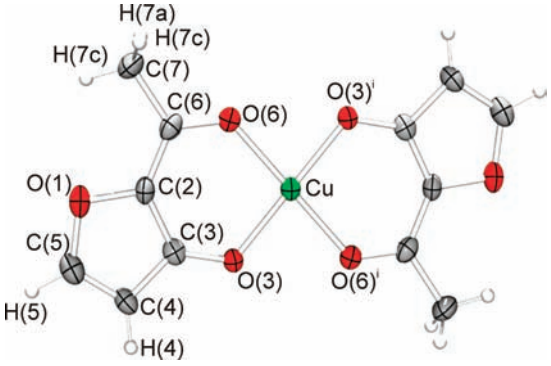

Figure 2. ORTEP representation of $[Cu(\mathbf{L}^2)_2]\cdot 8H_2O$ shown with 50% probability ellipsoids. Water molecules are removed for clarity.

The OH function [O(3)−H(3)] acts as a hydrogen-bond donor interacting moderately with the ketone oxygen [O(6)^{i}] from an adjacent molecule. Along with additional weak hydrogen bonds between the isomaltol molecules, this results in a three-dimensional (3D) arrangement within the lattice (see Figures S1−S3 and Table S2 in the Supporting Information).

Structure of $[Cu(\mathbf{L}^2)_2]\cdot 8H_2O$. Dark-green crystals of sufficient quality for X-ray analysis were isolated after the slow evaporation of an aqueous solution of the complex over several days. The structure confirms that isomaltol deprotonates upon complexation and forms a neutral complex with two six-membered chelate rings involving coordination of the copper(II) ion to the deprotonated hydroxy group [O(3)] and ketone [O(6)] oxygen atom of each ligand (Figure 2).

The copper(II) center adopts a pseudo-square-planar geometry with unremarkable Cu−O bond lengths and angles (Table 1). The conformation of each $\mathbf{L}^2$ anionic ligand contrasts with that observed in the X-ray structure of $\mathbf{HL}^2$. Compared to isomaltol alone, the C(2)−C(6) bond is rotated 180°.

Adjacent complexes show a weak C−H···O hydrogen bond similar to that observed in the structure of $\mathbf{HL}^2$ (Figure 3). The former interaction is indicated by a C(5)−H(5)···O(1) distance of 2.71 Å and results in the formation of a one-dimensional ribbonlike arrangement, which extends along the crystallographic *a* axis. In addition to this weak hydrogen bond, two solvent water molecules [O(10)] act as hydrogen-bond donors interacting with one of the chelating oxygen-donor atoms [O(3)] (Table 2 and Figure 3), leading to a water cluster, as described later.

The ribbonlike chains stack on top of each other with Cu−C(2) separations of 3.13 Å, suggesting the presence of copper furan π-stacking interactions between ribbons (Figure 4); related Cu−π system contacts have been reported previously for other copper(II) complexes containing unsaturated ligands.[20−22,40] Such π-stacking interactions seem to fall into the category of "metalloaromaticity" of a metal−heterocyclic chelate ring.[41]

Table 1. Selected Bond Lengths (Å) and Angles (deg) for $[Cu(\mathbf{L}^2)_2]\cdot 8H_2O$[a]

Cu−O(3)	1.90	O(3)−Cu−O(6)	96
Cu−O(3)^{i}	1.90	O(3)−Cu−O(6)^{i}	84
Cu−O(6)	1.94	O(3)^{i}−Cu−O(6)	84
Cu−O(6)^{i}	1.94	O(3)^{i}−Cu−O(6)^{i}	96
Cu−C(2)	3.13	O(3)^{i}−Cu−O(3)	180
Cu−Cg(1)	3.12	O(6)−Cu−O(6)^{i}	180
Cu−plane O(1) to C(5)	3.37		

[a] Symmetry operator: i, $-x-1, -y+1, -z$.

Details of relevant interatomic bond lengths and angles for the present system are listed in Table 2. The Cu−π interactions, together with the weak hydrogen-bonding interactions described above, result in the formation of infinite layers, which extend into the *ac* plane (Figure 5).

The chelate rings of one layer are connected by a hydrogen-bonding network involving an eight-water-molecule cluster (Figure 6). The water molecule containing O(11) is involved in three hydrogen-bonding interactions, while each of the others is involved in four such interactions (Table 2). A view along the *c* axis shows a diagonal layer of the octameric water cluster (Figure 7, left) illustrating the twisted strands present. Each ring in this layer is connected to its neighboring ring via 10 hydrogen-bonding interactions. Each water cluster is involved in two hydrogen bonds to the next diagonal layer (Figure 7, right; Figure S4 in the Supporting Information). Furthermore, the overall arrangement includes both five- and six-molecule hydrogen-bonded rings and is to some extent reminiscent of the structure of ice.[42] However, it needs to be noted that three of the water molecules [O(11), O(12), and O(13)] are disordered in the structure.

(40) (a) Franks, W. A.; Van der Helm, D. *Acta Crystallogr., Sect. B* **1971**, *27*, 1299–1310. (b) Van der Helm, D.; Tatsch, C. E. *Acta Crystallogr., Sect. B* **1972**, *28*, 2307–2312. (c) Clegg, J. K.; Lindoy, L. F.; Moubaraki, B.; Murray, K. S.; McMurtrie, J. C. *Dalton Trans.* **2004**, 2417–2423. (d) Clegg, J. K.; Lindoy, L. F.; McMurtrie, J. C.; Schilter, D. *Dalton Trans.* **2006**, 3114–3121.

(41) (a) Masui, H. *Coord. Chem. Rev.* **2001**, *219−221*, 957–992. (b) Castiñeiras, A.; Sicilia-Zafra, A. G.; González-Pérez, J. M.; Choquesillo-Lazarte, D.; Niclós-Gutiérrez, J. *Inorg. Chem.* **2002**, *41*, 6956–6958. (c) Janiak, C.; Chamayou, A.-C.; Royhan Uddin, A. K. M.; Uddin, M.; Hagen, K. S.; Enamullah, M. *Dalton Trans.* **2009**, 3698–3709. (d) Craven, E.; Zhang, C.; Janiak, C.; Rheinwald, G.; Lang, H. *Z. Anorg. Allg. Chem.* **2003**, *629*, 2282–2290. (e) Monfared, H. H.; Kalantari, Z.; Kamyabi, M.-A.; Janiak, C. *Z. Anorg. Allg. Chem.* **2007**, *633*, 1945–1948.

(42) Yoshizawa, M.; Kusukawa, T.; Kawano, M.; Ohhara, T.; Tanaka, I.; Kurihara, K.; Niimura, N.; Fujita, M. *J. Am. Chem. Soc.* **2005**, *127*, 2798–2799.

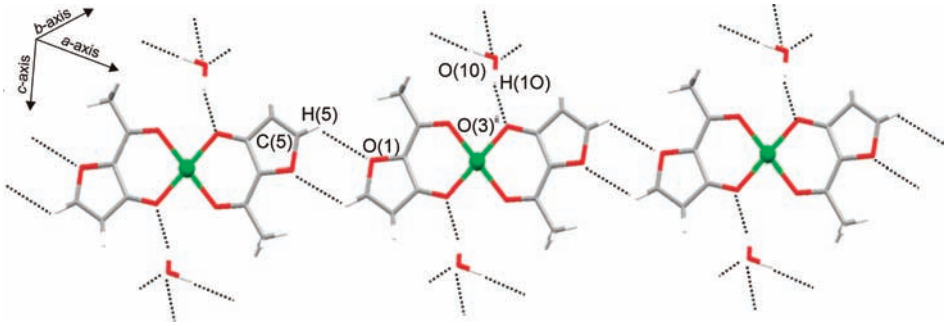

Figure 3. Ribbonlike arrangement formed by hydrogen bonding between adjacent complexes in $[Cu(\mathbf{L^2})_2]\cdot 8H_2O$. Dashed lines indicate hydrogen bonds.

Table 2. Hydrogen Bond Lengths (Å) and Angles (deg) in $[Cu(\mathbf{L^2})_2]\cdot 8H_2O$[a]

D	H	A	D−H	H···A	D−A	D−H−A
C(5)	H(5)	O(1)	0.95	2.71	3.37	127
O(10)	H(1O)	O(3)^{i}	0.91	1.96	2.80	154
O(10)	H(2O)	O(13)^{ii}	0.98	1.94	2.75	138
O(11)	H(3O)	O(10)	0.98	1.87	2.84	171
O(11)	H(4O)	O(12)	0.91	1.86	2.77	174
O(11)	H(4OA)	O(12)^{iii}	1.01	1.82	2.79	160
O(12)	H(5O)	O(12)^{iv}	0.86	1.92	2.78	173
O(12)	H(6O)	O(13)	0.83	1.99	2.76	153
O(12)	H(6OA)	O(11)^{v}	0.99	1.82	2.79	164
O(13)	H(8OA)	O(12)	0.89	1.88	2.76	169
O(13)	H(8O)	O(13)^{vi}	0.84	1.94	2.76	168
O(13)	H(7O)	O(10)^{vi}	0.98	1.84	2.75	153

[a] Symmetry operators: i, $-x, -y+1, -z$; ii, $-x+1, -y+1, -z+1$; iii, $x+1, y, z$; iv, $-x, -y, -z+1$; v, $x-1, y, z$; vi, $-x, -y+1, -z+1$.

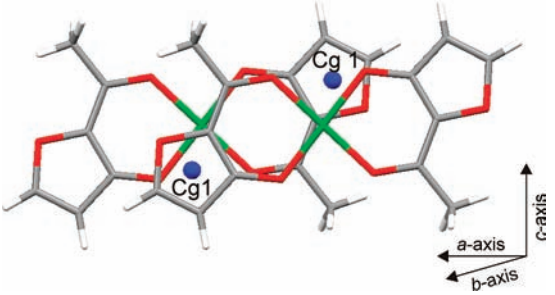

Figure 4. View of the molecular structure of $[Cu(\mathbf{L^2})_2]\cdot 8H_2O$ perpendicular to the plane of the furan ring showing the relationship between adjacent layers in terms of the aromatic π stacking involving copper(II).

In recent years, different water clusters have been identified in crystal hydrates that include both cyclic and acyclic structures;[43] only a few of those are octameric clusters.[44] The water cluster within the lattice of the bis(isomaltolato)copper(II) complex observed here is a further example of the rare cyclic octameric arrangement of water molecules.[45]

Protonation and Stability Constants. The hydrolysis constants for copper(II) and zinc(II) were determined as log $\beta_{10-2} = -13.46$ and -15.44, respectively. These values are in accordance with literature values.[6] In both cases, it was not possible to identify log β_{10-1} because of interference from the hydrolytic behavior of these metal ions.

The equilibrium constants for the protonation and complex formation of isomaltol with copper(II) and zinc(II) are given in Table 3, together with relevant literature data. For comparison, the protonation and stability constants for maltol with copper(II) and zinc(II) are also included in Table 3.

Speciation diagrams for the present systems are presented in Figure 8. In agreement with the literature, the stronger acidity of isomaltol is reflected by lower log K values for both protonation and complex formation. While for the complexes of isomaltol with copper(II) and maltol with copper(II) and zinc(II), the individual species distributions depend strongly on the pH value, in the case of isomaltol and zinc(II), the two species $[Zn(\mathbf{L^2})]^+$ and $[Zn(\mathbf{L^2})_2]$ formed coexist over a broad pH range (see Figure 8).

Only approximate stability constants were obtained for isomaltol complexation with iron(III) because the hydrolysis constants for these metal ions were unable to be determined with sufficient accuracy under the present conditions. However, from the experimental data it can be concluded that log β_3 is approximately 13.

DFT Calculations. As mentioned already, copper(II)−aromatic π-stacking interactions of the type observed in the present study (see Figures 4, 5, and 9) have not generally been recognized as an important structural motif in the chemistry of copper(II) complexes. Dispersion forces have been proposed previously[22] to provide the primary source of the binding in such systems rather than, say, electrostatic forces. The observed copper(II) interaction with a bound isomaltolate anion observed in the crystal structure of $[Cu(\mathbf{L^2})_2]\cdot 8H_2O$ provided a means to further investigate this. With this in view, we have performed DFT calculations on $[Cu(\mathbf{L^2})_2]$ stacked dimers and tetramers whose structures were based on the X-ray crystallographic results. For comparison, parallel calculations

(43) (a) Ludwig, R. *Angew. Chem., Int. Ed.* **2001**, *40*, 1808–1827. (b) Naskar, J. P.; Drew, M. G. B.; Hulme, A.; Tocher, D. A.; Datta, D. *CrystEngComm* **2005**, *7*, 67–70. (c) Liu, Q.-Y.; Xu, L. *CrystEngComm* **2005**, *7*, 87–89. (d) Janiak, C.; Scharmann, T. G. *J. Am. Chem. Soc.* **2002**, *124*, 14010–14011. (e) Zhuge, F.; Wu, B.; Liang, J.; Yang, J.; Liu, Y.; Jia, C.; Janiak, C.; Tang, N.; Yang, X.-J. *Inorg. Chem.* **2009**, *48*, 10249–10256. (f) Zhuge, F.; Wu, B.; Dong, L.; Yang, J.; Janiak, C.; Tang, N.; Yang, X.-J. *Aust. J. Chem.* **2010**, *63*, 1358–1364.

(44) (a) Blanton., W. B.; Gordon-Wylie, S. W.; Clark, G. R.; Jordan, K. D.; Wood, J. T.; Geiser, U.; Collins, T. J. *J. Am. Chem. Soc.* **1999**, *121*, 3551–3552. (b) Sun, Y.-Q.; Zhang, J.; Ju, Z.-F.; Yang, G.-Y. *Aust. J. Chem.* **2005**, *58*, 572–577. (c) Ma, B.-Q.; Sun, H.-L.; Gao, S. *Chem. Commun.* **2005**, 2336–2338. (d) Prasad, T. K.; Rajasekharan, M. V. *Cryst. Growth Des.* **2006**, *6*, 488–491. (e) Ghosh, S. K.; Bharadwaj, P. M. *Inorg. Chim. Acta* **2006**, *359*, 1685–1689.

(45) (a) Atwood, J. L.; Barbour, L. J.; Ness, T. J.; Raston, C. L.; Raston, P. L. *J. Am. Chem. Soc.* **2001**, *123*, 7192–7193. (b) Sun, C.-Y.; Zheng, X.-J.; Li, W.-J.; Wang, M.-W.; Fang, C.-Y. *Z. Anorg. Allg. Chem.* **2008**, *634*, 2663–2669.

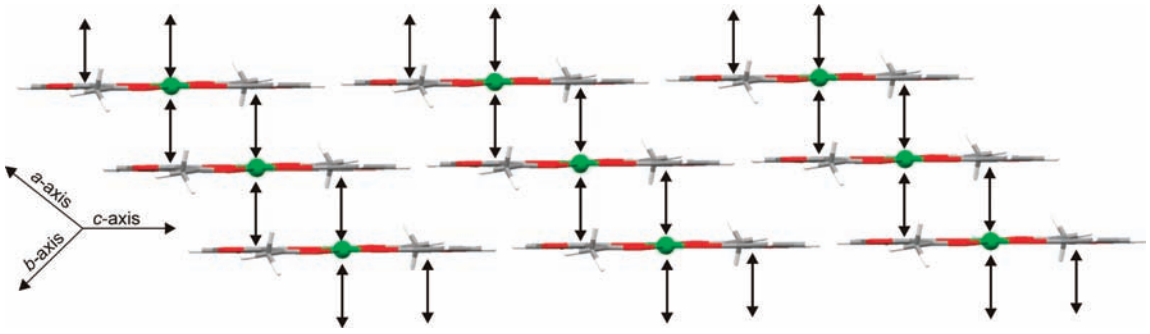

Figure 5. Representation of the layers that form through hydrogen bonding (including the water cluster) and the Cu−π interactions with the furan ring of $\mathbf{HL^2}$. The latter are indicated by arrows.

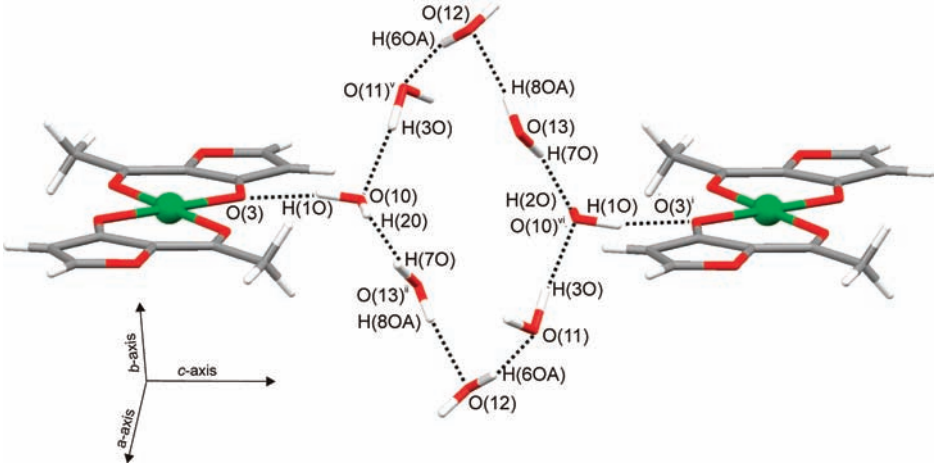

Figure 6. Representation of the connection between two complex molecules via hydrogen bonds involving eight solvent water molecules forming an eight-membered ring (disordered hydrogen atoms are omitted for clarity).

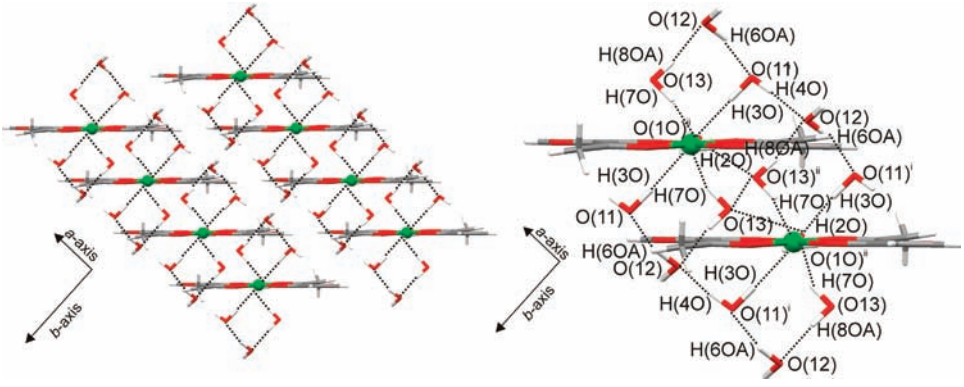

Figure 7. View along the *c* axis (left) and connection between the water clusters (right), showing the stacking of the aromatic planes.

Table 3. Protonation and Stepwise Stability Constants for Isomaltol $\mathbf{HL^2}$ and Maltol $\mathbf{HL^1}$ with Copper(II) and Zinc(II) [298 K; I = 0.15 M (KNO_3)]

	isomaltol		maltol		
	log K_1	log K_2	log K_1	log K_2	log K_3
H	5.63 (0.03) 5.64[14] 5.63[14] 5.55[15]		8.32[14] 8.67[46]		
Cu	5.04 (0.08)	4.57 (0.21)	7.89[46]	6.55[46]	
Zn	3.36 (0.04)	3.07 (0.08)	5.56[47]	4.75[47]	2.27[47]

on a previously reported analogous interaction between (neutral) benzene and [Cu($\mathbf{L^3}$)$_2$] (R = H, Scheme 2) have also been undertaken. The latter is a model complex based on the structure of the analogous complex [Cu($\mathbf{L^3}$)$_2$] with R = perfluorophenyl reported by Hori and Arii.[20] All optimized structures are shown in Figure 9.

The results of the gas-phase calculations for the [Cu($\mathbf{L^2}$)$_2$] stacked dimer (see Figure 9a) predict an interlayer spacing of 3.00 Å and a dimerization energy of −16.9 kcal·mol^{-1}, changing to 3.12 Å and −18.1 kcal·mol^{-1}

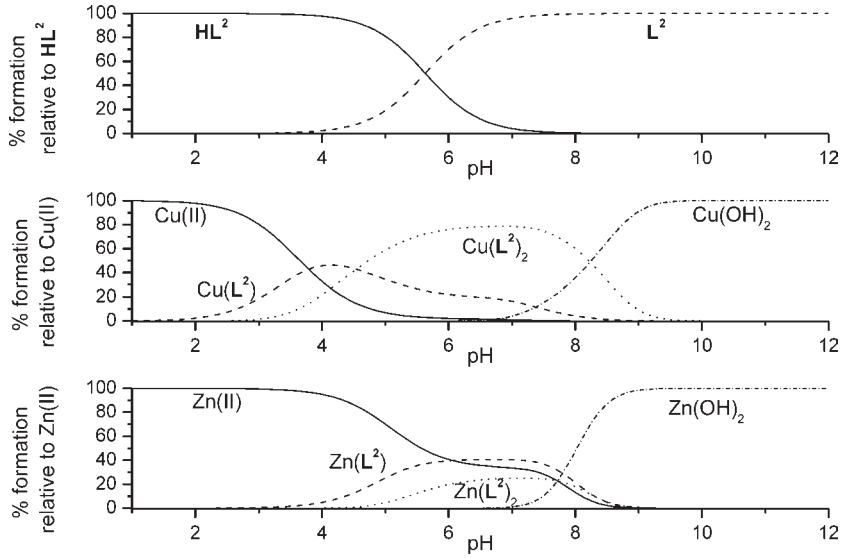

Figure 8. pH dependence of the species distribution for isomaltol (top) and its copper(II) (middle) and zinc(II) complexes (bottom). $c(Cu^{2+}) = c(Zn^{2+}) = c(\mathbf{HL^2}) = 5 \times 10^{-4}$ M in 0.15 M KNO_3 at 298 K.

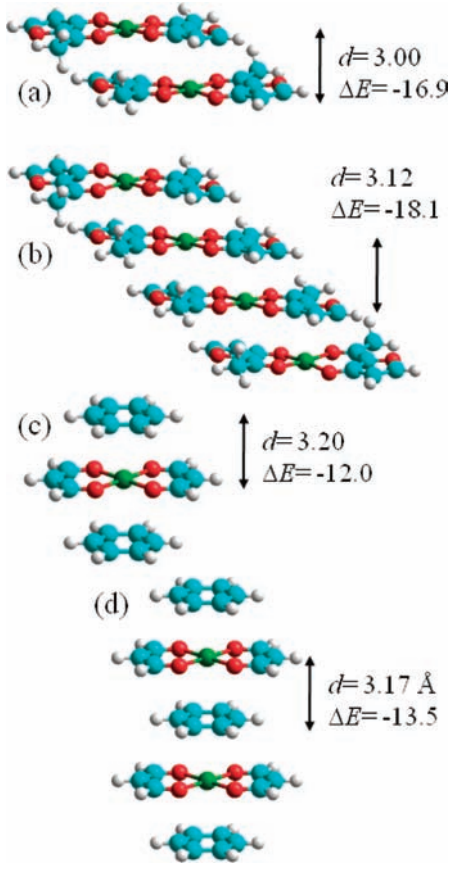

Figure 9. Calculated structures, showing interlayer distances d, in Å, and layer cleavage energies, ΔE, in kcal·mol^{-1}, for (a) a $[Cu(\mathbf{L^2})_2]$ stacked dimer, (b) a $[Cu(\mathbf{L^2})_2]$ stacked tetramer, (c) stacked model system $[Cu(\mathbf{L^3})_2]\cdot 2C_6H_6$, and (d) stacked model system $2[Cu(\mathbf{L^3})_2]\cdot 3C_6H_6$.

when the corresponding stacked tetramer is considered (Figure 9b). These distances appear to be converging well toward the observed value of 3.13 Å in the crystal structure, and there is a small collective effect on the binding energy. Note that here the interlayer

Scheme 2

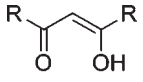

HL^3

interactions are between copper(II) ions and deprotonated (copper bound) isomaltolate anions, and so significant electrostatic polarization effects might possibly be anticipated.

The calculations for three and five layers of the model system in which analogous copper(II) ions in $[Cu(\mathbf{L^3})_2]$ (R = H) stack with neutral benzene rings are shown in Figure 9c,d. Similar interlayer separations are predicted (3.17−3.20 Å), but these are somewhat shorter than the value of 3.46 Å observed for the corresponding derivative with perfluorophenyl substituents;[20] this could simply be an indication of steric effects in the observed crystal but could also indicate that the calculations overestimate polarization and van der Waals effects.

The calculated binding energy changes only slowly with increasing layer numbers (−12.0 and −13.5 kcal·mol^{-1} for three and five layers, respectively) and is just 4−5 kcal·mol^{-1} less exothermic than those involving metal-bound ligand anions. While electrostatic effects are identified as being present, dispersion forces are shown to be dominant. This result is in agreement with the conclusions of Helios et al. obtained considering dispersion-corrected and -uncorrected DFT as well as MP2 calculations on a similar copper(II)−π interaction with a C=C double bond of a uracil ring.[22]

All binding energies shown in Figure 9 are corrected for BSSE; these corrections are found to be 2.0−2.6 kcal·mol^{-1} for the model system and 3.4−4.5 kcal·mol^{-1} for $[Cu(\mathbf{L^2})_2]$. All possible spin multiplicities arising from combinations of copper(II) ions were considered in the calculations, and only the lowest-energy structures, which all exhibit ferromagnetic coupling, are reported.

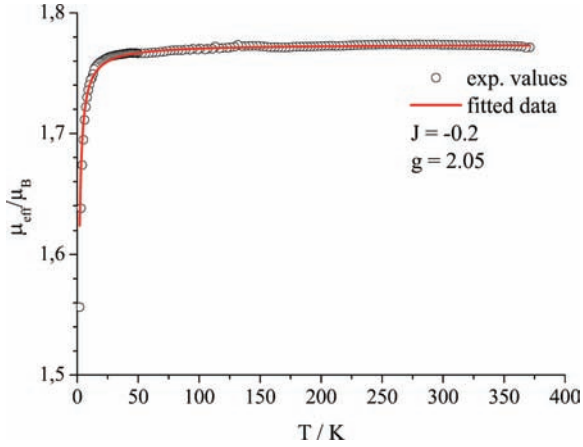

Figure 10. Experimental data (circles) from a variable-temperature (2−371 K) magnetic study and their theoretical fits (red line) using the Bonner and Fischer model[48] for spin $^1/_2$ Heisenberg chains.

Magnetic Study. A variable-temperature magnetic study was performed in order to determine the magnetic properties of [Cu($\mathbf{L^2}$)$_2$]. The experimental data from such measurements are shown in Figure 10 and a fitted curve under the assumption of equally spaced and antiferromagnetically coupled spin $^1/_2$ Heisenberg chains of copper(II).

The Hamiltonian for the isotropic interaction is given by

$$H = -J\sum_{i=1}^{n-1} S_{Ai}S_{A(i+1)}$$

and the molar susceptibility is given by the numerical expression

$$\chi = \frac{Ng^2\beta^2}{kT}\frac{0.25+0.074975x+0.07235x^2}{1.0+0.9931x+0.172135x^2+0.757825x^3}$$

$$x = \frac{|J|}{kT}$$

developed by Bonner and Fisher.[48]

A least-squares fit of the temperature-dependent magnetic susceptibility data reveals the presence of very weak antiferromagnetic exchange interactions between the copper(II) ions with a value for the magnetic exchange coupling constant J of -0.2 cm^{-1} and a g value of 2.05.

In contrast to the calculated ferromagnetic behavior for the defined dimeric or tetrameric model structures just discussed, the crystalline material consists of infinite chains that are linked by a hydrogen-bond network, including via water clusters. Hence, as observed for a related system,[49] the influence of long-range antiferromagnetic exchange interactions via the above noncovalent intermolecular linkages seems likely to account for the observed difference between the calculated and experimental results for the magnetic exchange behavior of this system.

Conclusions

In this study, we have investigated the solid-state-, solution-, and gas-phase interaction of copper(II) with isomaltol and shown it to form a bis-ligand species of the type [Cu($\mathbf{L^2}$)$_2$]. The stability of this copper complex is significantly lower than that obtained with the isomeric maltol ligand. A complex of similar stoichiometry but lower stability is formed with zinc(II). Because of isomaltol's weak complex formation with these two metal ions, we expect, at most, only a slight influence on the in vivo uptake of copper and zinc. Thus, isomaltol is unlikely to be responsible for the observed effect of MRPs on the in vivo metal uptake mentioned earlier.

Apart from the possible biological implications just mentioned, the structure of the [Cu($\mathbf{L^2}$)$_2$] complex appears to be of particular intrinsic interest. This species crystallizes to yield an interesting 3D solid-state array in which the molecules are held together in two-dimensional planes by hydrogen bonding that also involves an eight-node water cluster along with other weak intermolecular interactions. The planes are stacked vertically via weak hydrogen bonds including the water cluster and copper(II) ligand−π interactions, with this unusual interaction predicted to be quite substantial at 18.1 kcal·mol^{-1}. Isolated examples of other interactions of this type involving neutral aromatic ligands have also been recognized previously[20,40] and from the present study are predicted to be only slightly weaker at ca. 14 kcal·mol^{-1}. In accordance with the results of Helios et al.,[22] this interaction type is concluded to be primarily dispersive in nature. Copper(II)−π interactions of this general type clearly have implications for interpreting the structures of particular copper-containing biological[50] and material systems as well as, for example, for modeling the catalytic properties of copper surfaces.[39]

Finally, the study serves to extend the known metal ion chemistry of isomaltol. It also further documents an additional noncovalent interaction type that has received little attention in the past. As such, this aspect of the study adds to the inventory of weak interactions necessary for the understanding (and ultimate prediction) of crystal packing in copper(II)-containing systems of the present type.

Acknowledgment. We thank the Deutsche Forschungsgemeinschaft, the Australian Research Council, and the IPDF Scheme (University of Sydney) for financial support and the National Computational Infrastructure of Australia for the provision of computational resources.

Supporting Information Available: Selected crystallographic data and further structural figures. This material is available free of charge via the Internet at http://pubs.acs.org. Data are also deposited in the Cambridge Crystallographic Data Centre (CCDC), deposition numbers CCDC 796735 ($\mathbf{HL^2}$) and CCDC 796736 {[Cu($\mathbf{L^2}$)$_2$]·8H$_2$O}. These data can be obtained free of charge via www.ccdc.cam.ac.uk/data_request/cif or e-mail data_request@ccdc.cam.ac.uk or by contacting The Cambridge Crystallographic Data Centre, 12 Union Road, Cambridge CB2 1EZ, U.K. (fax +44 1223 336033).

(46) Gerard, C.; Hugel, R. P. *C. R. Acad. Sci.* **1982**, *295*(Series II), 175–177.
(47) Gerard, C.; Hugel, R. P. *J. Chem. Res. Synop.* **1978**, *10*, 404–405.
(48) Bonner, J. C.; Fisher, M. E. *Phys. Rev. A* **1964**, *135*, 640–658.
(49) Choudhury, S. R.; Lee, H. M.; Hsiao, T.-H.; Colacio, E.; Jana, A. D.; Mukhopadhyay, S. *J. Mol. Struct.* **2010**, *967*, 131–139.
(50) Yorita, H.; Otomo, K.; Hiramatsu, H.; Toyama, A.; Miura, T.; Takeuchi, H. *J. Am. Chem. Soc.* **2008**, *130*, 15266–15267.